Sensor System to Capture Spatial & Temporal Pressure Distribution from Ballistic Impact Helmet Backface Deformation

L. Voo[1], A. Lurski[1], A. Veith[1], E. Butler[1], J. Marcus[1], Q. Luong[1], and M. Kleinberger[2]

[1]*The Johns Hopkins Applied Physics Laboratory (JHU/APL), 11100 Johns Hopkins Rd, Laurel, MD, USA*
liming.voo@jhuapl.edu
[2]*U.S. Army Combat Capabilities Development Command Army Research Laboratory, Aberdeen Proving Ground, MD, USA*

Abstract. Limited knowledge of the spatial and temporal pressure distribution over the course of body armour and helmet back-face deformation during a ballistic impact is a significant impediment in developing effective injury metrics and better protective systems for countering behind helmet blunt trauma (BHBT). This knowledge gap can largely be attributed to the lack of viable solutions to measure the contact pressure distributions with minimal interference at the interface between the human surrogate and the armour system. JHU/APL has recently developed a spatially integrated thin-film stress sensor array system to address this experimental measurement gap. The packaged system prototype is only 0.20mm (0.008inch) thick and could easily fit between the human surrogate and armour. A version of the system with 13 stress sensors has been tested on and below the impact pad of the Adaptable Testing and Load Assessment System (ATLAS) Headform using an air-cannon propelled projectile that simulated the impact momentum and shape of a helmet back-face deformation during a non-penetrating ballistic impact. The prototype sensor system proved to be capable of surviving, sensing high-speed pressure response, and producing quality signals under severe mechanical insults. The spatial and temporal distributions of the resulting impact pressure were captured during high-speed loading conditions. The sensor spatial distribution density of the current prototype can be increased by including more individual stress gauges or custom-designing more stress-sensing elements. This new sensing capability could enable more precise measurement of the injurious loading conditions behind the helmet and body armour, and thereby improve performance evaluation of personal protective equipment. Further development of this technology will include exploration of its capabilities, spatial resolution, and pressure measurement accuracy, under ballistic BHBT conditions.

1. INTRODUCTION

Combat helmets are designed to stop the bullets from penetrating the helmet shell, and therefore mitigating the risk of ballistic penetrating injuries to the head. It has been well documented that the rapid deformation of the helmet back-face, without complete ballistic penetration, can still cause significant injuries to the head, including severe skull fractures [1-3]. This phenomenon is commonly referred to as Behind-Helmet Blunt Trauma (BHBT). Several studies have attempted to investigate different injury mechanisms and injury risk curves using simulated back-face deformation impactors [4-5]. The apparent differences in the resulting skull fracture patterns in these studies (with and without helmet), however, may be a result of different contact pressure distributions, which have not been measured experimentally [6].

Several studies have attempted to investigate stress conditions under BHBT conditions [2, 7-9]. Ommaya et al. estimated impact stress values for adult human skull fracture to be 43 MPa [7]. Other studies calculated mean stress at 50% risk of skull fracture to be 15 MPa to 51 MPa [2] based on analysis of strains from cadaveric skull fractures and match-paired anthropomorphic test dummy tests. On the other hand, computational modelling and simulation of the BHBT mechanisms also reported calculated stresses on the skull tissues [8-9]. Although such numerical results are useful for parametric assessments and qualitative understanding of the effect various variables on BHBT related stresses in the head, the simplified bone geometry and lack of tissue level model validation make quantitative prediction of tissue stresses uncertain. The validity of such calculated estimates remains a gap due to lack of a suitable sensing system to measure the contact stress experimentally.

The current method of assessing BHBT injury risk of various combat helmets is based on residual plastic deformation left in clay [10-11], with the assumption that the deformation depth correlates to skull fracture risk. The existing biomechanical data on skull fracture are often reported in terms of peak impact force magnitude depending on the impactor profile [12]. An alternative assessment method for skull fracture that could utilize force measurement would provide a more scientifically supported injury

https://doi.org/10.52202/081621-0037

correlate for BHBT risk assessment. A multi-location test head surrogate, the Adaptable Testing and Load Assessment System (ATLAS) Headform, was developed by the Johns Hopkins Applied Physics Laboratory (JHU/APL) to collect behind helmet impact force responses for helmet BHBT performance assessment [13,14]. Other impact force-based head surrogates include multiple load cells, such as the seven-cell Ballistic Load Sensing Headform (BLSH) [15-18] and the 17-cell Pk17dynA [19,20] that enable measurement of force distribution at a fixed impact location [19,20] or locations [13-18]. While excellent repeatability and reproducibility is a great advantage of such load-cell based measurement systems [21], they are limited by the lack of deformation in the direction of impact, which a human skull possess, and fixed measurement locations. It is, therefore, desirable to have a dynamic surface contact stress sensing system for BHBT testing with minimum deformation resistance in the direction of impact and ability to measure at any location on a head surrogate.

This paper describes a prototype thin-film stress sensing system custom-designed and fabricated to measure dynamic contact pressure spatial and temporal distribution under BHBT environment. Its experimental usability, ability to survive such harsh mechanical conditions, and sensing capabilities are demonstrated through simulated BHBT testing in the laboratory.

2. MATERIALS AND METHODS

The ATLAS Headform [13] was employed as the human surrogate in this study (Figure 1). Its surface represents that of human head anatomy. Response is measured by a high-capacity load cell (Model 224C, PCB Piezotronics, Depew, New York, USA) supported by a metal shaft on the back and covered by a steel cap (Impact Cap) surface (Figure 1a). The Impact Cap is also covered by a polymer Impact Pad (Shore 40A hardness neoprene rubber). A critical challenge of developing the thin-film stress sensing system is its form factors that allows it to fit between the helmet and the test headform, as well as between the headform Impact Pad and Impact Cap (Figure 1). There is a very limited space on the Impact Cap area for the packaged sensing system to fit (Figure 1b). The total thickness of the sensing system package, besides the wires, needs to be less than 0.254mm (0.01inch).

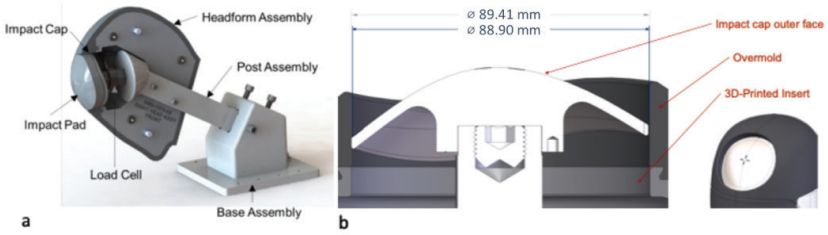

Figure 1: (a) Cross-sectional view of the ATLAS Headform (frontal impact module); (b) Cross-sectional view of the Impact Cap and its surrounding

The individual thin-film piezoelectric polyvinylidene fluoride (PVDF) stress sensor from Dynasen (PVF2 11-0.040-EK, Dynasen Inc., Goleta, CA, USA) was selected to construct the thin-film sensing system for BHBT contact pressure spatial and temporal distribution measurement. It has high stress sensing capacity range (10-10,000MPa), rapid response (nanosecond), very thin, and a long-thin form factor (Figure 2).

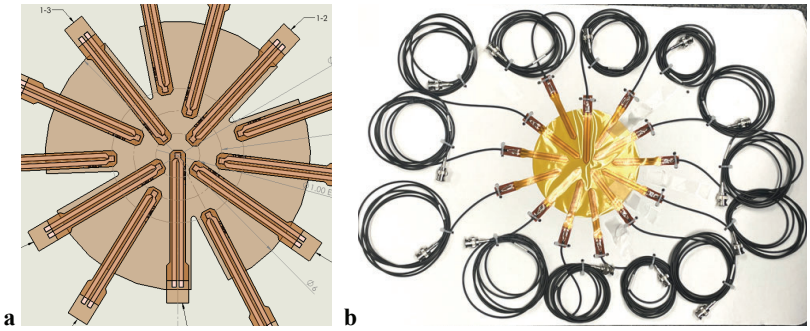

Figure 2: Packaged pressure sensing system with fixed sensor layout (a) and cables (b)

The PVDF sensor used in this study produces an electrical potential proportional to the mechanical stress on its material surface. It can be used as a force sensor or stress sensor depending on how the electrical signals are converted into the values in an engineering unit and how the contact area is accounted. In this study, it is used as a stress sensor with a very small sensing element and assumed uniform stress distribution within the sensing element area. Each individual stress sensor is supplied with a static calibration value while its dynamic calibration data is obtained using an equation provided by Dynasen Inc. Similar PVDF sensors have a track record of being used in blast and ballistic impact conditions [22,23]. The sensing element sizes (PVF2 11-0.040-EK) adopted for this project were 1.016mm×1.016mm (0.04inch x 0.04inch). The placement design of the stress sensors considered the shape and size of the helmet back-face deformation as well as potential spatial distribution gradient: the contact pressure is expected to be greatest at the impact centre and decreasing radially from the centre. In this initial design, the sensor placement covered the total potential compressive stress area induced by the impact projectile which has a 62mm diameter. The individual stress sensors, therefore, were packaged concentrically starting with one sensor at the expected impact centre and four sensors in each of the three concentric rings at distances of 12.7mm, 25.4mm, and 38.1mm (0.5inch, 1.0inch, and 1.5inch) from the centre (Figure 2a). It was expected that the compressed area behind the Impact Pad would be slightly greater than the projectile diameter due to pad deformation. The sensor locations were fixed with adhesive and sandwiched between two layers of thin films with a total thickness of 0.2032mm (0.008inch). The whole sensor system package can fit into the ATLAS Headform sensing area on top of the Impact Cap and covered by the Impact Pad (Figure 3a). The non-sensing area of the hardware, including the cables (Figure 2b), could be routed through the backside of the ATLAS Headform load cell and exit the side (Figure 3b and 3c).

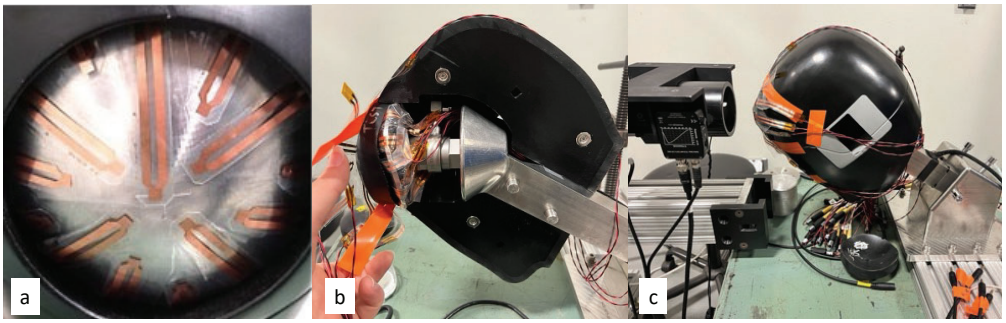

Figure 3: Packaged thin-film pressure sensing system fitted into the ATLAS Headform: (a) on the load cell cap; (b) with cables wrapped around the back; and (c) on the Impact Pad and ready for testing

BHBT impact conditions were simulated using an air-cannon driven projectile impactor representing the bullet-helmet mass and deformation shape. This cylindrical projectile has a spherical front surface, 192g mass, and 62mm (2.45inch) diameter. A pressure-velocity curve was developed to determine the appropriate pressure for the desired projectile velocities. Two lasers at the end of the barrel 10 cm (3.94inch) apart act as a velocity gate to measure the velocity of the projectile immediately before impact. The impact velocities used in the experiments,15, 23, 30, and 45 m/s (50, 75, 100, and 150 ft/s), enabled evaluation of the thin-film sensor system over a BHBT severity range.

Eleven simulated BHBT tests were conducted on the front impact location of the ATLAS Headform, with the thin-film stress sensing system installed below the Impact Pad and another on top of it (Figure 3c). The sequence of the tests was: 3 tests at 15 m/s (50 ft/s), 3 tests at 30 m/s (100 ft/s), 1 test at 15 m/s (50 ft/s), 1 test at 23m/s (75ft/s), and 3 tests at 45 m/s (150 ft/s). The signals from the stress sensors and the ATLAS load cell were recorded at a sampling rate of 200 kHz using a DEWETRON Inc. data acquisition system (DEWE-801, Orion MDAQ-V200, East Greenwich, RI, USA). No post-test data filtering was applied for the data analysis.

3. RESULTS

3.1. Sensor System Conformity to Curve Surface

The sensor system fit condition on the curved surface of the impact cap was assessed at the front impact location of the ATLAS Headform using both visual inspection and computed tomography (CT)

https://doi.org/10.52202/081621-0037

imaging approaches. CT scans of ATLAS Headform with and without sensor installation were obtained. Although not apparent from the visual inspection, the CT images demonstrated that the sensor system could fit within the curved gap space with no noticeable gap increase between the Impact Pad and the Impact Cap surface. Note, to eliminate artifacts from the CT scanner, a 3D printed polymer Impact Cap was used instead of the steel Impact Cap.

3.2. Sensor System Survivability under BHBT Test Environment

With some iterative design improvements, the pressure sensing system based on PVDF stress sensor proved to be capable of surviving the air-cannon–simulated BHBT impacts. All the PVDF sensors produced expected signals in repeated tests. The earlier tests (prior to the test series reported here) caused damage to the sensor outside the Impact Pad at the impact centre under the most severe impact condition (45 m/s). Covering the sensor package with two additional layers of thin films prevented such damage. In addition, one connector on the outside sensor package was separated from the sensor due to large deformation during the most severe test condition (45 m/s) in this test series.

3.3. Temporal Contact Stress Distribution Measurement

The stress sensing system produced signals that did not require post-test signal filtering. No signal clipping was ever observed. The following event response times of the tests can be identified (Figure 4): initial impact contact with the outside centre stress sensor, load cell response initiation, load cell signal peak, Impact Pad full compression, end of projectile contact, peak Impact Pad expansion, and Impact Pad recovery. Those event-times were identified based on analysis of high-speed video images, load cell response signal, and signals from individual stress sensors. The positive values in the figures represent compressive stress (or positive pressure) while the negative values represent tensile stress (or negative pressure). The projectile contact initiated the response of the outside centre stress sensor response, followed by the signal initiation of the inside centre stress sensor and load cell (Figure 4).

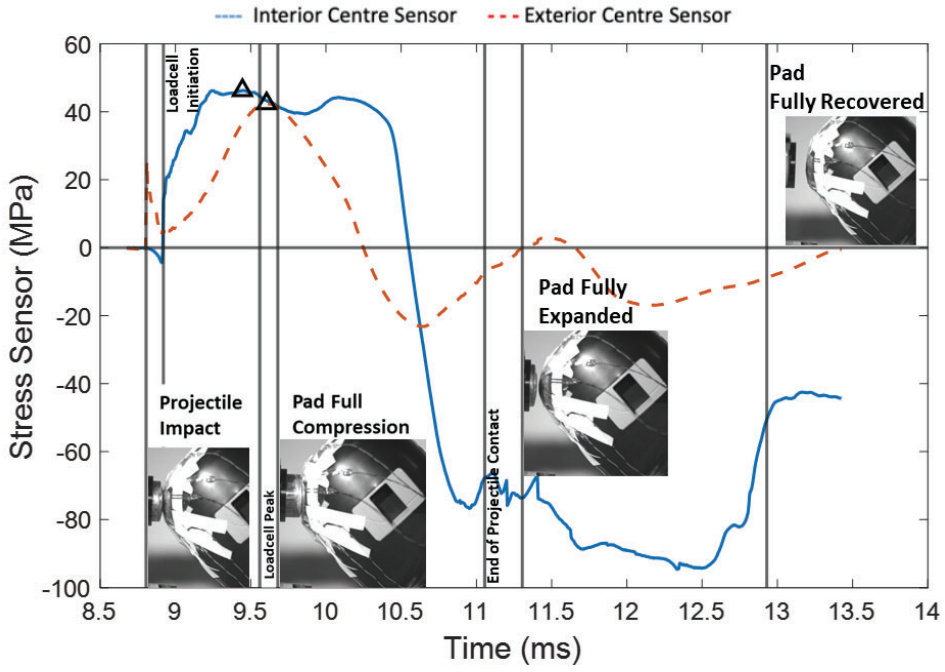

Figure 4: Event times illustrated on centre stress sensor signals inside and outside the Impact Pad (Note: positive values indicate compressive stress while negative values indicate tensile stress)

The initiation of the off-centre signal came after the centre signal and also from the exterior sensors to the interior sensors (Figure 5). The timing of signal peaks varied depending on the impact velocity. A tensile stress was observed inside the Impact Pad during the projectile rebound phase (Figure 4), consistent with what was observed in high-speed video.

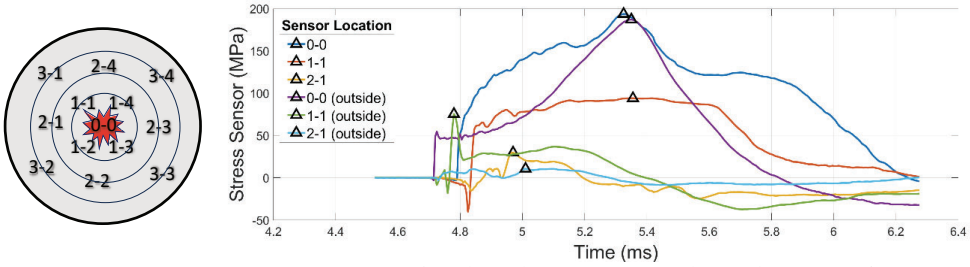

Figure 5: Contact stress responses at locations (impact centre to ring 2) from a 30m/s test

Figure 6 illustrates the force or peak pressure time from when the projectile crossed the laser velocity gate for each test. The mean peak pressure times, averaged from multiple repeat tests, are shown along with their corresponding standard error. The peaks occurred at the same time at the centre and peripheral locations with minimum difference between inside and outside of the Impact Pad and the load cell in any given test. In general, the peak time decreased as the projectile impact velocity increased.

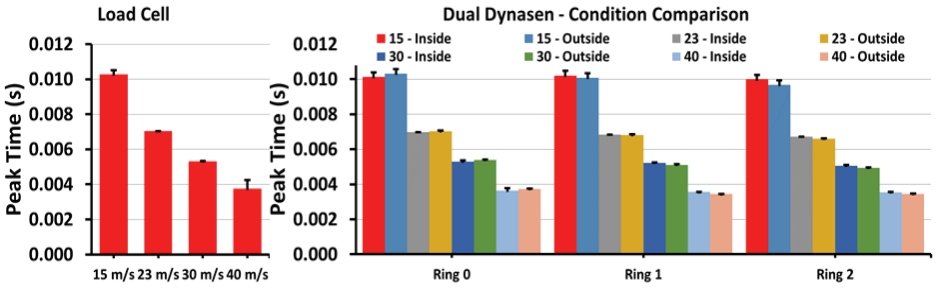

Figure 6: Peak times of force and contact stress signals at various locations (ring 0, ring 1, ring 2) inside and outside the Impact Pad at different velocities

3.4. Spatial Contact Stress Distribution Measurement

The force and pressure response peaks increased as the impact velocity increased (Figure 7). In general, the peak contact pressure was higher inside the Impact Pad than the outside. This difference, however, diminished or even reversed as the impact velocity increased. The peak contact pressure was also greater at the impact centre (Ring 0) and decreased with the distance away from the centre (Ring 1 and Ring 2).

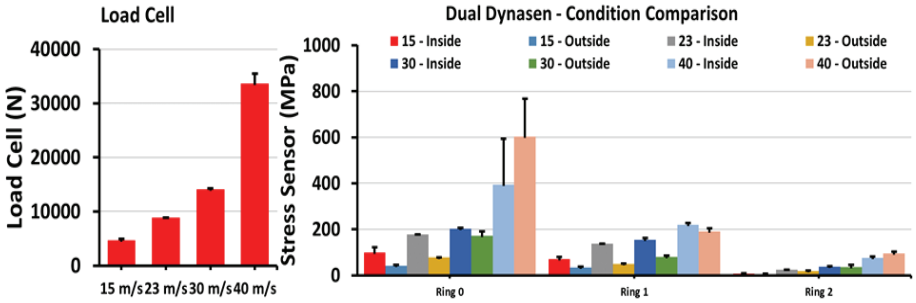

Figure 7: Effect of impact velocity on peak response force and contact stress peak at different distances from the impact centre (Ring 0) to more peripheral locations (Rings 1 and Ring 2)

https://doi.org/10.52202/081621-0037

Heat maps of contact pressure inside and outside of the Impact Pad were created to explore their distribution pattern change over time at different velocities (Figure 8). The greatest amount of contact pressure is concentrated in the centre and the first ring of the sensing area for both the sensor placed on the inside and outside of the pad across all velocities. The pressure maps show little response beyond the projectile frontal contact surface, which is captured by the centre and first two rings of sensors, even though the peripheral sensors in ring 2 did produce low readings because of Impact Pad deformation. Figure 8 also shows the effect of the impact velocity on the pressure pattern inside and outside the impact pad.

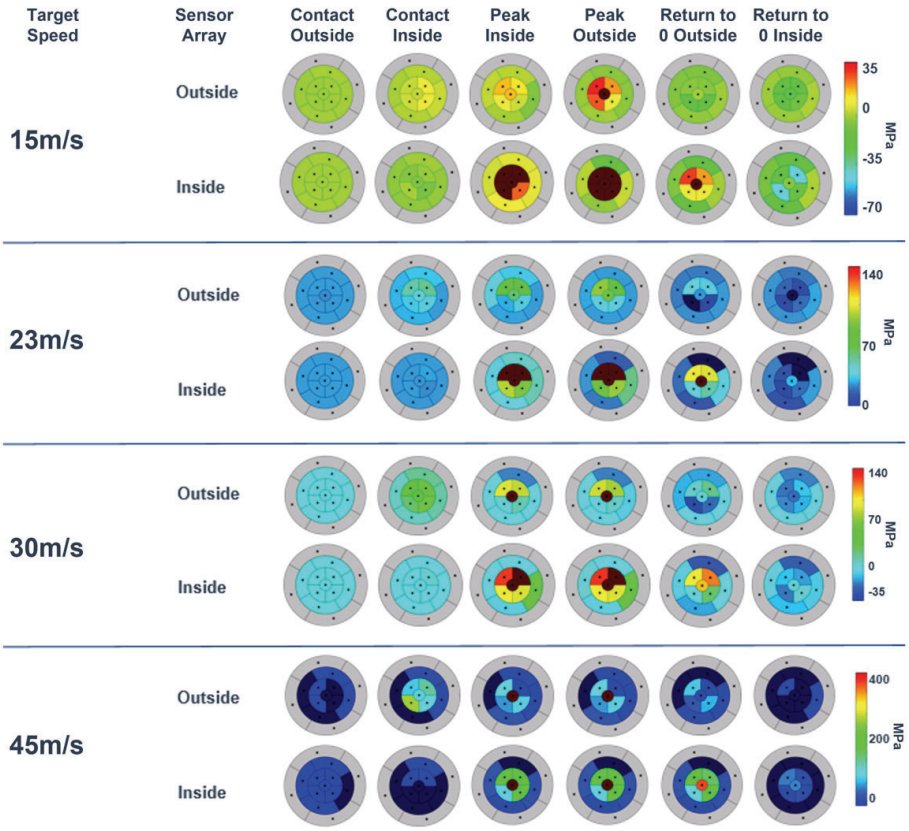

Figure 8: Contact stress patterns at distributed locations, impact progression time, and different impact velocities

3.5. Detecting Impact Pad Damping Capability Change

The thin-film pressure sensing system was able to detect the effect of degradation of the polymer Impact Pad on impact pressure transmission (Figure 9). To compare across different tests of the same target velocity, time zero of the response signal was established to be when the centre outside sensor crossed a threshold that correlated with projectile contact initiation. The centre contact pressure response inside the Impact Pad showed progressively higher peak values from the first, second, third, and seventh test of a test series (figure 9a). The peak transmitted pressure from the 7th test was more than three times that of the first test. The differences in the force responses did not show such a progressive change, instead showing the effect of projectile velocity variation (Figure 9b).

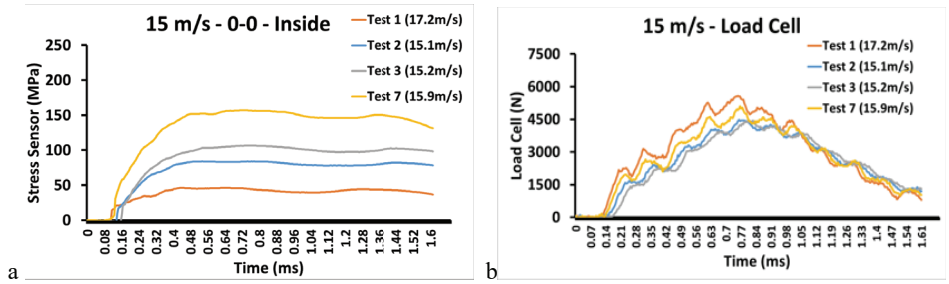

a b

Figure 9: The interior centre stress responses (a) and ATLAS Headform load cell force response (b) from the first, second, third, and seventh test of a test series

A deeper dive analysis of the contact pressure inside the Impact Pad demonstrated more granular pressure measurement capability of this sensing system (Figure 10). The contact pressures at the four locations on ring 1 were similar to each other and the centre pressure location (ring 0) (Figure 10, left) while the pressures at the four more peripherical locations (ring 2) were much lower. The loading damping and distributing effect of the Impact Pad was dramatically reduced after sustaining three tests of six tests (Figure 10 right). Two of the ring-1 gauges sensed much greater pressure than in the first test. The pressure at the impact centre (A00) now increased the greatest and reflected the most prominent surface at that location. The pressures at more peripheral locations (A12-A24) did not show meaningful increase in pressure magnitude.

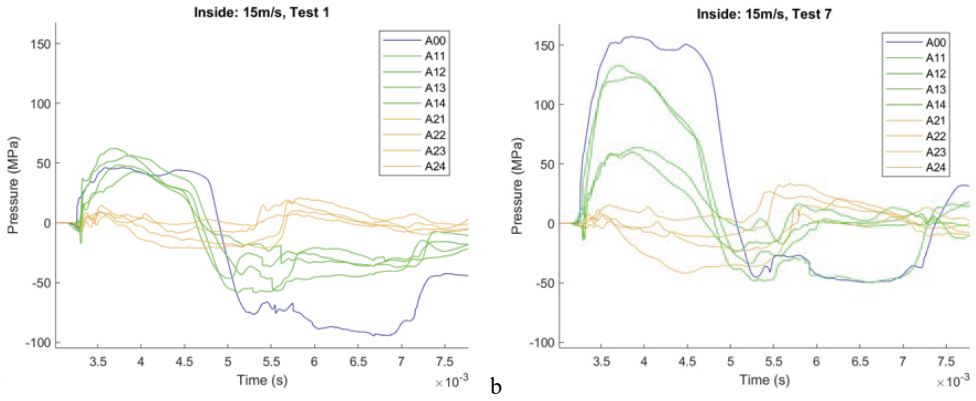

a b

Figure 10: The inside contact pressures at the impact centre (A00), near centre (A11-A14) and more peripheral (A21-A24) from the first test (a) and the 7th test (b) at the same velocity

4. DISCUSSION

The feasibility and capability of measuring contact pressure distribution spatially and temporarily under BHBT impact conditions was investigated using the JHU/APL prototype thin-film stress sensor package. The experimental testing employed the ATLAS Headform as the human head surrogate, while simulated BHBT impacts were generated by an air-cannon propelled projectile. The contact pressure measurement leveraged a custom-designed thin-film stress-sensor system fitted into and over the ATLAS Headform Impact Pad at the front impact location. The experimental results demonstrated that such a sensor system 1) can survive BHBT relevant test conditions; 2) can be fitted into the ATLAS Headform without need for hardware modification; 3) produces low noise stress signals; and 4) allow analysis of contact pressure distribution patterns and magnitude change over the duration of the impact. Additionally, the measurements are able to assess the effect of impact severity and impactor shape.

The packaged thin-film stress sensor system was shown to be able to sustain simulated BHBT impacts repeatedly with minimum damage if sufficient caution and protection were implemented. The sensor package damage around the centre sensor was determined to be the result of the extreme stress. Subsequent tests, which produced the data for the analysis of this study, demonstrated that such damage could be mitigated with additional protective layers of thin-film material applied to the

https://doi.org/10.52202/081621-0037

potentially damaged area. Damage occurred at the connection between the sensor wire strip and the extension wires on sensors installed outside the Impact Pad as a result of the large deformation of the Impact Pad. Such damage could also be prevented with additional cable slack during the sensor system installation.

The response forces measured by the ATLAS load cell are consistent with range of BHBT mechanical environment reported in the literature [4,14,24]. Iwaskiw produced BHBT skull fractures using post-mortem human subject (PMHS) heads in live-fire tests and conducted matched-pair test on the ATLAS Headform which measured forces in the range of 9.6 - 22.6 kN (2.2 – 5.1 klbf) [14] and impulse in the range of 2.62 to 3.81 Ns. Raymond reported mean peak force of 5.8 kN from BHBT skull fracture experimental study using a projectile impact to the lateral side of PMHS head [4]. Daniel reported mean projectile impact force ranges of 12.3, 6.3, and 21.6 kN (2.8, 1.4, and 4.9 klbf) for impacts to the front, side and rear of PMHS head, respectively that produced skull fractures [24]. The current study produced headform response forces in the range of 4.5 - 33.0 kN (1.0 - 7.4 klbf) (Figure 7) which spans those of the BHBT test conditions reported in the BHBT literature.

The response contact pressures measured by the thin-film stress sensor system are consistent with the expected outcomes for the test conditions and sensor locations. The measured contact pressure at each sensor location increased progressively as the impact velocity increased. The measured pressure generally decreases as the sensor location further away from the impact centre. The pressures from the thin-film sensors backed by a rigid steel surface (Impact Cap of the load cell) are mostly higher than those backed by the Impact Pad (Figure 7), consistent with the boundary stiffness effect.

The thin-film stress sensor system has sufficient sensitivity to even detect local padding material degradation due to repeated impact and surface geometry effects (Figures 9 and 10). Such effects cannot be observed visually nor easily analysed using the single load cell signal in ATLAS headform. This capability is particularly useful for BHBT and BABT applications, as injury risk in such scenarios largely depend on the local loading conditions and affected by the surface geometry and local stiffness of the head. The ability to detect changes in the test system that could affect injury prediction would be critical for performance evaluation of personal protective equipment. A spatially distributed sensing system, such as the thin-film stress sensor system in this study, demonstrated such capabilities. Test headforms with multicell rigid load cells such as BLSH (7-cell) [15-18] and Pk17dynA (17-cell) [19,20] may be able to measure such pad damping changes as well, although such result has not been reported in the open literature. On the other hand, the thin-film sensing system also has the advantages of being used in any surface location of a human surrogate while not resisting deformation in the direction of impact loading. Increasing the spatial density of the stress sensor system (more sensing elements in a given area) could further improve its local measurement resolution and accuracy, and is technically feasible.

The contact stresses measured by the thin-film stress sensors on the ATLAS Headform surface and below the Impact Pad are in the same order of magnitude as those reported in the BHBT biomechanics literature. The compact skull bone stress estimated by finite element analysis studies ranged 55 – 80 MPa (7977 – 11603 psi) depending on suspension pad stiffness in BHBT conditions [8]. Similarly, skull bone stress was reported to range 75 – 89 MPa (10877 – 12908 psi) depending on the velocity of the bullet impacting the helmet [9]. The experimental skull fracture stress under impact was reported to be on average 43 MPa (6237 psi) [7] or estimated to be 51 MPa (7397 psi) [2]. The surface stresses in the central area (25.4mm diameter circle) of this study were 34 – 175 MPa (4931 – 25382 psi) outside and 69 – 209 MPa (10008 – 30313 psi) inside the Impact Pad (Figure 7). However, these stress quantities are likely not of the same form or location and therefore should be used for reference of order of magnitude rather than for direct comparison. Nevertheless, this comparison further supports the utility of this thin-film sensor system for BHBT contact pressure measurement application. Additional research could enable quantitative BHBT risk assessment based on stress-related injury metrics.

The impact test conditions in this study adopted a well-established method for producing BHBT skull fractures using air-cannon launched impact projectiles to simulate the impact of the helmet back face on the head during the ballistic impact [4,5,24]. The impact energy and velocity used in such studies represent the helmet back face rather than those of the striking bullet which are expected to be much higher. The projectile impact energy range of 4.4 to 31.3 J in this study is comparable to the range of 5 to 40 J reported in the two experimental studies using cadaveric specimens [5,24]. The projectile impact velocity range of 15 to 45 m/s in this study spans another cadaveric study's 18 to 37 m/s velocity range [4]. However, such experimental test method may not replicate all aspects of the BHBT conditions important for BHBT injury mechanisms and/or helmet performance. For example, the impact velocity range used in projectile impact testing may only represent the lower bound of those in the deforming helmet back face in a helmeted ballistic impact under BHBT conditions. The non-

rigid and progressively changing shape of the deforming helmet back face could be critical factors for contact pressure distribution and injury mechanism that are not simulated in the tests using the projectiles. Therefore, the pressure distribution results from this study may not represent the true BHBT conditions of the helmeted human head. Nevertheless, those results do demonstrate the measurement potential of such thin-film stress sensor system to enable better understanding of the biomechanical factors associated with BHBT injuries and developing more effective injury correlation metrics. Future evaluation of the thin-film stress sensor system under helmeted BHBT test conditions would be valuable and more definitive for its intended application.

The current prototype of this thin-film stress sensor system can be further improved. Increasing spatial sensing density could improve measurement of pressure gradients in the critical area and capture more precisely the surface geometry effect between different locations of the head. The number of sensing elements in this study is largely limited by the project scope and budget. Doubling the stress gauge density is feasible without requiring change in the gauge design. Custom-designed stress sensing grid for the targeted BHBT and BABT application could be done to optimize sensing performance, test operation, and cost. The current prototype has only been tested under simulated BHBT conditions using an air-cannon propelled projectile, and needs to be evaluated under live-fire ballistic testing with a helmet system to fully demonstrate its utility. Further development of this technology will include exploration of its capability, spatial resolution, and pressure measurement accuracy under ballistic BABT/BHBT conditions.

5. CONCLUSION

The prototype thin-film stress sensor system, which was designed to fit onto head surrogates and enable additional measurements of the spatial distribution of BHBT loading, proved to be capable of surviving, sensing high-speed pressure response, and producing quality signals under severe simulated BHBT impact conditions. The spatial and temporal distributions of the impact pressure were captured during such high-speed loading conditions and comparable to those expected in BHBT loadings. The spatial sensor density of the current prototype can be increased by including more individual stress sensors or by custom-designing more stress-sensing elements. This new sensing capability could enable more precise measurement of the injurious loading conditions behind the helmet and body armour, and thereby improve performance evaluation of personal protective equipment.

Acknowledgments

This research effort was supported by the U.S. Army Combat Capabilities Development Command Army Research Laboratory (DEVCOM ARL). Any opinions, findings and conclusions or recommendations expressed in this material are those of the author(s) and do not necessarily reflect the views of DEVCOM ARL.

References

[1] A. W. Carroll and C. A. Sonderstrom, "A new nonpenetrating ballistic injury," *Annals of surgery,* vol. 188, no. 6, p. 753, 1978.

[2] Bass, C.R., B. Boggess, B. Bush, M. Davis, R. Harris, M.R. Rountree, S. Campman, J. Ecklund, W. Monacci, G. Ling, G. Holborow, E. Sanderson, and S. Waclawik. “Helmet Behind Armor Blunt Trauma.” Paper presented at the RTO Applied Vehicle Technology Panel/Human Factors and Medicine Panel Joint Specialists’ Meeting held in Koblenz, Germany, May 19-23, 2003.

[3] K. A. Rafaels, et al. "Injuries of the head from backface deformation of ballistic protective helmets under ballistic impact," *Journal of forensic sciences,* vol. 60, no. 1, pp. 219-225, 2015.

[4] D. Raymond, Van Ee ., et al. "Tolerance of the Skull to Blunt Ballistic Temporo-Parietal Impact," *Journal of biomechanics,* vol. 45, no. 12, pp. 2479-2485, 2009.

[5] C. A. Weisenbach, et al. "Preliminary Investigation of Skull Fracture Patterns Using an Impactor Representative of Helmet Back-Face Deformation," *Military medicine,* vol. 183, pp. 287-293, 2018.

[6] Y. Li,, Adanty K., et al. "Review of Mechanisms and Research Methods for Blunt Ballistic Head Injury," *Journal of biomechanical engineering,* vol. 145, no. 1, 2023.

[7] Ommaya, A.K., W. Goldsmith, L.E. Thibault. “Biomechanics and neuropathology of adult and paediatric head injury.” British Journal of Neurosurgery 16(3):220-242, 2002.

[8] Li X., Gao X., Kleiven S. “*Behind helmet blunt trauma induced by ballistic impact: A computational model*.” International Journal of Impact Engineering. Vol 91 (2016) 56–67, 2016.

[9] Cai Z., Huang X., Xia Y., et al. “*Study on Behind Helmet Blunt Trauma Caused by High-Speed Bullet*.” Applied Bionics and Biomechanics, Article ID 2348064, 2020.

https://doi.org/10.52202/081621-0037

[10] U.S. Department of Justice, National Institute of Justice Standard for Ballistic Helmets National Institute of Justice, NIJ 0107.01, 2024.
[11] National Research Council (U.S.) Committee on Testing Armor Materials, "Testing of Body Armor Materials: Phase III." National Academies Press, Washington, DC., 2012.
[12] Goldsmith W. and Monson K.L., "The State of Head Injury Biomechanics: Past, Present, and Future, Part 2: Physical Experimentation." Crit Rev Biomed Eng, 33 (2005), 105-207.
[13] M. M. Trexler, et al. "Development of a Modular Load-Sensing Headform," in *Personal Armour Systems Symposium*, Washington D.C., 2018.
[14] Iwaskiw A., Howes C., Hingorani R., Bradfield C., Mazuchowski E., Clark M., Luong Q., Drewry D. Loads Associated with Behind Helmet Blunt Trauma: Matched-Pair Load Sensing Headform Tests Correlated with Skull Fracture Severity. Personal Armour Systems Symposium, Dresden, Germany, 2023.
[15] Anctil B., Bourget D., Pageau G. Rice, K. and Lesko J. "Evaluation of Impact Force Measurement Systems for Assessing Behind Armour Blunt Trauma for Undefeated Ballistic Helmets." Personal Armour Systems Symposium, Hague, The Netherlands, 2004.
[16] Bolduc, M, Anctil, B. Improved Test Methods for Better Protection, a BABT Protocol, Proposal for STANAG 2920, Personal Armour Systems Symposium, Quebec, Canada, 2010.
[17] Philippens M.M.G.M., Anctil B., Markwardt K.C., Results of a Round Robin Ballistic Load Sensing Headform Test Series. PASS 2014, London, UK, 8th-12th September 2014, pp.
[18] Philippens M., BABT protection for composite ballistic helmets; Ballistic Load Sensing Headform & Suspension System; TNO report TNO2014 R10151, Technical Sciences, P.O. Box 2280 AA Rijswijk, The Netherlands, 2014.
[19] Grobert S., Gedon H., Peschel O. "Development of a Test Setup for an Integrated Assessment of Ballistic Backface Deflections on Combat Helmets." *Personal Armour Systems Symposium*, Amsterdan, Netherland, 2016.
[20] Grobert S., Gedon H., Peldschus S., Peschel O. "Comparative Tests with Pk17dynA for an Integrated Assessment of Ballistic Backface Deflections on Combat Helmets." *Personal Armour Systems Symposium*, Washington D.C., 2018.
[21] Voo L., Swetz S., Luong Q., Warfield J., Alvarez B., Brinkley K., O'Donnell J., Bevan M., Merkle A. "Improved Repeatability and Reproducibility of the Ballistic Load Sensing Headform." Personal Armour Systems Symposium, Amsterdan, Netherland, 2016.
[22] Tanaka S., Hokamoto K., et al. "High-velocity impact experiment of aluminum foam sample using powder gun." *Measurement* 44, 2185–2189, 2011.
[23] Bartyzak S. and Mock W. "Characterization of viscoelastic materials for low-magnitude blast mitigation." J Physics: Conference Series 500 (2014) 182003.
[24] Daniel R., Rooks T., Gomez J., et al. "Evaluation of Skull Fracture Risk Associated with Helmet Back-Face Deformation." USAARL-Tech-FR—2022-24, 2022.